Cadmium and calcium uptake in isolated mitochondria-rich cell populations from the gills of the freshwater rainbow trout

Fernando Galvez, Denise Wong and Chris M. Wood

Am J Physiol Regulatory Integrative Comp Physiol 291:170-176, 2006. First published Feb 9, 2006;
doi:10.1152/ajpregu.00217.2005

Am J Physiol Regul Integr Comp Physiol 291: R170–R176, 2006.
First published February 9, 2006; doi:10.1152/ajpregu.00217.2005.

Cadmium and calcium uptake in isolated mitochondria-rich cell populations from the gills of the freshwater rainbow trout

Fernando Galvez, Denise Wong, and Chris M. Wood
Department of Biology, McMaster University, Hamilton, Ontario, Canada

Submitted 28 March 2005; accepted in final form 24 January 2006

Galvez, Fernando, Denise Wong, and Chris M. Wood. Cadmium and calcium uptake in isolated mitochondria-rich cell populations from the gills of the freshwater rainbow trout. *Am J Physiol Regul Integr Comp Physiol* 291: R170–R176, 2006. First published February 9, 2006; doi:10.1152/ajpregu.00217.2005.—A novel cell isolation technique was used to characterize cadmium and calcium uptake in distinct populations of gill cells from the adult rainbow trout (*Oncorhynchus mykiss*). A specific population of mitochondria-rich (MR) cell, termed the PNA^+ MR cell (PNA is peanut lectin agglutinin), was found to accumulate over threefold more ^{109}Cd than did PNA^- MR cells, pavement cells (PV cells), and mucous cells during a 1-h in vivo exposure at 2.4 μg/l ^{109}Cd. In vitro ^{109}Cd exposures, performed in standard PBS and Cl^--free PBS, at concentrations from 1 to 16 μg/l ^{109}Cd, were also carried out to further characterize Cd^{2+} uptake kinetics. As observed during in vivo experiments, PNA^+ MR cells accumulated significantly more ^{109}Cd than did other cell types when exposures were performed by an in vitro procedure in PBS. Under such conditions, Cd^{2+} accumulation kinetics in all cell types could be described with Michaelis-Menten relationships, with K_m values of ~3.0 μg/l Cd (27 nM) for both MR cell subtypes and 8.6 μg/l Cd (77 nM) for PV cells. In similar experiments performed in Cl^--free conditions, a significant reduction in ^{109}Cd accumulation in PNA^+ MR cells was seen but not in PNA^- MR or in PV cells. In vitro ^{45}Ca fluxes were also performed to determine the cellular localization of Ca^{2+} transport in these functionally distinct populations of gill cells. ^{45}Ca uptake was most pronounced in PNA^+ MR cells, with levels over threefold higher than those found in either PNA^- MR or in PV cells. Results from the present study suggest that the PNA^+ MR cell type is a high-affinity and high-capacity site for apical entry of Cd^{2+} and Ca^{2+} in the gill epithelium of rainbow trout.

freshwater fish gill epithelium; peanut lectin agglutinin; metal binding; MINEQL+

CADMIUM, AS FREE ionic Cd^{2+}, is particularly lethal to fish in low waterborne concentrations. In freshwater fish, toxicity of the metal is generally associated with impairment of active Ca^{2+} transport in fish by the competitive blockade of epithelial Ca^{2+} channels or noncompetitive inhibition of high-affinity Ca^{2+}-ATPase transporters in the gill epithelium (29, 30). The antagonistic interaction between the uptake of waterborne Ca^{2+} and Cd^{2+} at the freshwater fish gill is well established (10, 24, 30, 31). Overall, there is strong evidence that these two ions share a common uptake mechanism on the fish gill. Hollis et al. (10) showed that Ca protects against Cd^{2+} uptake in freshwater rainbow trout by causing a decrease in Cd^{2+} accumulation at the gills as waterborne Ca concentration is increased. Similarly, Wicklund and Runn (32) have found that ^{109}Cd uptake is decreased in the gills of fathead minnows (*Phoxinus phoxinus*) if waterborne Ca concentration is elevated. Reciprocally, increased waterborne Cd leads to impairment of internal Ca balance (33).

On the basis of almost entirely correlative evidence, it is thought that the mitochondria-rich (MR) chloride cell of the gill epithelium is the primary cell type in the fish gill implicated in the uptake of these two ions from water (14, 15, 18, 22). Perry and Wood (22) found that proliferation of MR cells on the gill epithelium of trout resulted in elevated rates of unidirectional Ca^{2+} uptake from water. Interspecies differences in Ca^{2+} uptake rates have also been correlated with the relative abundance of MR cells on the fish gill, as assessed by electron microscopy (19). Additional evidence has been obtained with surrogate models of the freshwater fish gill, such as the opercular epithelium of the killifish (13) and tilapia (15) and the cleithrum skin of rainbow trout (13), tissues containing an abundance of MR cells that are thought to be analogous to those found on the freshwater fish gill. In these studies, a strong correlation between active Ca^{2+} uptake and MR cell density was also found. Despite the almost general consensus that MR cells are involved in Ca^{2+} transport, there are a number of studies questioning this general transport model. Isihara and Mugiya (11) and Wicklund Glynn et al. (31) have shown a heterogeneous pattern of Ca^{2+} and/or Cd^{2+} accumulation in MR cells, suggesting the presence of functionally distinct MR subtypes in the fish gill. It has even been proposed with autoradiographic techniques that ^{109}Cd is transported across the entire gill epithelial surface, rather than specifically in MR cells (34). Interestingly, in this same study, ^{45}Ca was found to localize to MR Cl^- cells, implicating this cell as the primary mediator of transepithelial Ca^{2+} uptake. However, the authors argued that ^{109}Cd might be taken up through nonspecific channels in pavement (PV) cells or that ^{109}Cd may be taken up through Ca^{2+} channels on PV cells, challenging the view that Ca^{2+} channels are restricted to MR cells.

The idea of functionally distinct MR cell subtypes has gained acceptance in recent years. Pisam et al. (23) described at least two MR cell subtypes in the freshwater gill of euryhaline fishes based on differences in surface morphology under scanning electron microscopy. However, until recently, it has been difficult to address the question of whether these proposed MR cell subtypes are, in fact, functionally distinct. To study this problem, recent studies have used differential staining of the fish gill with peanut lectin agglutinin (PNA) to identify at least two MR cell subtypes (3, 4, 6, 24). This lectin histochemical approach of identifying MR cell subtypes was subsequently combined with density centrifugation and magnetic cell sorting techniques to isolate enriched populations of these MR cells, as well as PV cells, from a dispersed gill cell population (4). One

Address for reprint requests and other correspondence: F. Galvez, Dept. of Biological Sciences, Louisiana State Univ., 264 Life Sciences Bldg., Baton Rouge 70803-1715 (e-mail: galvezf@lsu.edu).

The costs of publication of this article were defrayed in part by the payment of page charges. The article must therefore be hereby marked "*advertisement*" in accordance with 18 U.S.C. Section 1734 solely to indicate this fact.

of the MR cell subtypes possesses features characteristic of traditional "chloride cells" (PNA^+ MR cells), whereas the other exhibits ultrastructural features similar to those of PV cells (PNA^- MR cells). More importantly, recent studies have shown these MR cells to have different roles in Na^+ transport and acid-base regulation (4, 25).

The gill cell isolation technique of Galvez et al. (4) allows us for the first time to assess the cellular localization of solute transport in the gill epithelium of freshwater fish. This approach should allow us to assess the relative importance of PV cells (34) and MR cells (11, 31) in Cd^{2+} and Ca^{2+} uptake. It also provides a unique method of examining whether a subpopulation of MR cells exists with enhanced Cd^{2+} and Ca^{2+} transport processes. Consequently, the primary objective of this study was to determine the uptake and distribution of waterborne Cd^{2+} and Ca^{2+} in the three aforementioned isolated gill populations. These studies will help gain further insight into the mechanisms of Cd^{2+} and Ca^{2+} transport in the freshwater fish gill, not only between PV cells and MR cells, but also between PNA^+ and PNA^- MR cell subtypes.

METHODS

Fish holding conditions. Adult rainbow trout (~150 g) were obtained from Humber Springs Hatchery (Orangeville, ON, Canada) and acclimated to flowing dechlorinated Hamilton tap water [Lake Ontario water; in mmol/l: 1.0 Ca, 0.6 Na, 0.7 Cl; in mg/l: 3.0 dissolved organic matter; and in milligrams per liter: 140 hardness (as $CaCO_3$); 95 alkalinity; pH 8.0, 12°C]. The trout were held in 400-liter tanks for 2 wk before experimentation and fed three times weekly to satiation with dry food pellets (Martin Mills, Tavistock, ON, Canada).

Isolation and fractionation of gill epithelial cells. Isolation and fractionation of the gill epithelial cells were performed with a modified version of the techniques developed by Galvez et al. (4). Trout (~150 g) were randomly selected and killed by an overdose of MS-222 (0.5 g/l; Syndel Laboratories, Vancouver, BC, Canada) followed by a cephalic blow. The entire gill basket was removed, and the individual arches were rinsed in PBS (in mM: 137 NaCl, 4.3 KCl, 4.3 Na_2HPO_4, 1.4 NaH_2PO_4) and blotted to remove congealed external blood and mucus. The gill tissue was cut into smaller sections and placed in a 50-ml polypropylene conical tube containing ~10 ml of ice-cold PBS. The gills were digested in 5 ml of 0.2 mg/ml collagenase (in PBS) (type 1A; Sigma, St. Louis, MO) and incubated at room temperature with vigorous agitation (300 rpm) for 8 min. The gills were passed through a transfer pipette ~50 times to promote further digestion. Afterward, the gill cells were filtered through 100-μm nylon cell strainers (BD Falcon, Bedford, MA) into 50-ml conical tubes containing ~20 ml of PBS. The entire digestion procedure was repeated once on the undigested gill filaments to increase the yield of dispersed gill cells.

After digestion with collagenase, dispersed gill cells were incubated in a red blood cell lysis buffer (in mM: 10 $KHCO_3$, 154 NH_4Cl, 0.1 Na_2·EDTA). After 1 min, the red blood cell lysis buffer was diluted approximately sixfold with PBS, and the gill cells were centrifuged at 500 *g*. After an additional wash step, pelleted cells were resuspended in 3 ml of PBS and placed on top of a 1.03 g/ml Percoll (Sigma) solution (pH 7.8) in a 15-ml conical tube and spun for 8 min at 1,000 *g*. The cells on top of the 1.03 g/ml Percoll solution consisted of mucocytes and some cellular debris (5). The cells settling to the bottom of the 1.03 g/ml Percoll solution were resuspended in 3 ml of PBS and placed on top of a 1.05 g/ml Percoll solution and spun again for 8 min at 1,000 *g*. The cells fractionating above the 1.05 g/ml Percoll gradient were the PV cells, whereas those pelleting to the bottom of the 1.05 g/ml Percoll gradient were the MR cells (5). This procedure, which has shown to be robust for isolating gill cells of different fish species, takes advantage of the inherently high density of mitochondria relative to other subcellular organelles, allowing MR cells to settle to the bottom of the 1.05 g/ml Percoll fraction, whereas the lower-density PV cells remain at the top of the same density gradient. In preliminary studies, it was found that cells fractionating to the bottom of the 1.05 g/ml Percoll gradient stained almost exclusively to the mitochondria-sensitive dye, Mitotracker-green FM (see Ref. 4 for staining protocol), as visualized by a laser confocol microscope (Radiance 2000; Bio-Rad, Hercules, CA) equipped with argon and helium-neon lasers with peak outputs of 488 and 543 nm. In comparison, cells at the top of the 1.05 g/ml Percoll gradient stained poorly to the mitochondria-sensitive indicator. The relative enrichments used here were quantitatively similar to those obtained in previous studies (4, 5), in which functionally viable PV and MR cells were separated from one another. All gill cell fractions were diluted to ~10 ml PBS and centrifuged at 500 *g* for 5 min. All Percoll centrifugations were performed with a swing-bucket-type rotor. The PV and mucous cells were resuspended in 1–2 ml of PBS (depending on total cell numbers) and left on ice until processed further. The MR cells were resuspended in 0.5 ml of 40 μg/ml PNA-biotin in PBS and incubated for 20 min on ice with periodic agitation. The cells were pelleted and washed once with 1 ml of PBS. The MR cells were resuspended in 1:50 dilution of streptavidin microbeads (Miltenyi Biotec, Auburn, CA) in PBS (total volume of 0.5 ml) and incubated for 15 min at 4°C with periodic agitation. The solution was pelleted at 500 *g* for 5 min, washed with 1 ml of PBS to remove any unbound microbeads, and respun at 500 *g* for another 5 min. The cells were fractionated into two distinct populations using a magnetic bead separation technique (MACS), according to the manufacturer's instructions. In short, cells were filtered through a 30-μm preseparation filter (Miltenyi Biotec) to remove cell clumps and passed directly into an iron column (MS+-type column) surrounded by a strong magnet (OctoMACS separation unit). While still being held within a magnetic field, each column was given 3 × 0.5-ml rinses with PBS. The cells eluting during these rinses were termed the PNA^- MR cells. An additional elution was performed after the column was removed from the magnetic field. These cells were termed the PNA^+ MR cells. All centrifugation steps were performed at 4°C. Aliquots of each cell population were stained with trypan blue, and live cells were counted with a hemocytometer and expressed as 10^6 cells/ml.

In vivo ^{109}Cd exposures. One-hour Cd exposures (2.4 ± 0.1 μg/l; $n = 11$ or 12) on intact trout were performed in 3 liters of dechlorinated Hamilton tap water with continuous aeration. The desired concentration of Cd was added entirely as ^{109}Cd (as $^{109}CdCl_2$, NEZ058; Perkin-Elmer, Boston, MA; 3.64 mCi/mg). Water samples were taken at 5 and 55 min from the start of the flux period and analyzed for gamma radioactivity (Minaxi Auto-Gamma 5000 series; Canberra Packard Instrument, Meriden, CT). The water samples were also acidified (0.5% HNO_3 acid) and analyzed for total Cd concentration by atomic absorption spectroscopy on a graphite furnace (Varian SpectraAA-220 with GTA-110 atomizer, Mulgrave, Australia). After the 1-h Cd exposure, fish were rinsed in flowing water for 20 min to remove superficially bound Cd. Isolated gill cell populations (PV cells and PNA^+ MR and PNA^- MR cells) were obtained as described previously.

Time series for in vitro ^{109}Cd exposures. A time series was performed to determine the optimum exposure time for subsequent in vitro ^{109}Cd fluxes. Because of the limited availability of PNA^+ MR cells (see RESULTS for details), these experiments were performed only with total MR cells (i.e., before separation on the magnetic column) and PV cells. Isolated gill cells were exposed to ^{109}Cd at 2, 4, 8, and 16 μg/l ^{109}Cd for 15, 30, 60, 120, 240, and 360 s (as $^{109}CdCl_2$; Perkin-Elmer; 3.64 mCi/mg) in 24-well cell culture plates. One-milliliter suspensions of gill cells were added to culture-plate wells; at the start of each flux, 1 ml of ^{109}Cd flux solutions (at two times the desired Cd concentrations) was added and then mixed by gentle pipetting. At each time point, a 0.25-ml aliquot of gill cell suspension

Table 1. *Cadmium speciation using MINEQL+*

Cd Species	PBS	Cl^--free PBS (1–8 μg/l Cd)	Cl^--free PBS (16 μg/l Cd)
Cd^{2+}	14.6%	83.1%	58.6%
$CdCl^+$	61.4%	N/A	N/A
$CdCl_{2(aq)}$	20.0%	N/A	N/A
$CdCl_3^-$	1.6%	N/A	N/A
$CdHCO_3^-$	N/A	1.0%	N/A
$CdCO_{3(aq)}$	N/A	4.6%	3.3%
Cd gluconate	N/A	11.1%	7.8%

Values are expressed as a percentage of the total Cd concentration. N/A, not available. Major dissolved Cd species at concentrations of Cd ranging from 1 to 16 μg/l in PBS and Cl^--free PBS were determined with the geochemical speciation program MINEQL+ (26).

was removed and collected on 0.45-μm nitrocellulose membrane filters (ME25 membrane filter; Schleicher & Schuell) connected to a vacuum manifold (Millipore, Bedford, MA). Filters were washed with ~10 ml of ice-cold PBS before being collected for gamma counting. Preliminary experiments demonstrated that this protocol was sufficient to remove any superficially bound ^{109}Cd from the surface of the cells. In subsequent in vitro ^{109}Cd fluxes, gill cells were fluxed for 60 s based on time-series results (data not shown). This time point was chosen based on the fact that accumulation was still on the linear part of the curve but only shortly before a plateau was reached.

In vitro ^{109}Cd exposures performed in standard PBS. Initial in vitro ^{109}Cd exposures were performed in standard PBS (see above for recipe) on PV, PNA^- MR, and PNA^+ MR cells at 1, 2, 4, 8, and 16 μg/l ^{109}Cd. After 60 s of ^{109}Cd exposure, fluxes were terminated as outlined in the previous section. Filters were washed with ~10 ml of ice-cold PBS before they were collected for gamma counting.

In vitro ^{109}Cd exposures performed in Cl^--free PBS. A series of in vitro ^{109}Cd exposures was performed in Cl^--free PBS, in which NaCl and KCl were replaced with equimolar concentrations of sodium gluconate and potassium gluconate. After fluxes, filters were washed with ~10 ml of ice-cold Cl^--free PBS before being collected for gamma counting. Otherwise, all procedures were identical to those described previously.

In vitro ^{45}Ca exposures performed in PBS. PV, PNA^-, and PNA^+ MR cells were isolated from control fish and exposed to varying concentrations of ^{45}Ca (as $^{45}CaCl_2$, NEZ013; Perkin-Elmer) for 30 min. Fluxing time was increased from those used in in vitro ^{109}Cd exposures to allow for adequate detection of radioactivity. Ca stocks at twice the desired concentrations were added to the cells to yield final Ca concentrations of 5, 10, 20, 50, or 100 μM. ^{45}Ca fluxes were terminated by filtering aliquots of gill cells through nitrocellulose filters. Filters were washed with PBS to remove superficially bound ^{45}Ca radioisotope. Filters were digested overnight in 1 ml HNO_3 acid, after which 10 ml Ultima Gold scintillation fluor (Perkin-Elmer) was added to each digest for beta counting (Tri-carb 2900TR liquid scintillation counter; Perkin-Elmer, Downers Grove, IL). Internal standardization demonstrated that quench was both constant and negligible; therefore, no correction for counting efficiency was necessary.

Analyses. Waterborne ^{109}Cd radioactivities (in cpm/ml) and total Cd concentrations (in ng/ml) in flux chambers were determined from the average radioactivities and total Cd concentrations measured at the beginning (time = 5 min) and end (time = 55 min) of the in vivo ^{109}Cd fluxing period. These measurements were used to calculate the average specific activities (in cpm/ng). Similarly, specific activities of the solutions used in the in vitro Cd^{2+} and Ca^{2+} fluxes were calculated, except that only samples at the beginning of fluxing periods were taken. Specific activities were used to convert radioactivity in isolated cells into picogram or nanogram values. These absolute uptake rates were then expressed per 10^6 cells.

Michaelis-Menten analyses (*Eq. 1*) of the relationships between ^{109}Cd burden (Cd_{in}) and Cd concentration ([Cd]) were used to calculate K_m and B_{max} (maximal binding) according to the following formula:

$$Cd_{in} = (B_{max} \times [Cd])/(K_m + [Cd]) \quad (1)$$

For PV cells and PNA^- MR cells (PBS treatment only), the program TableCurve 2D (version 5.01) was used to subtract a small nonsaturable, linear Cd^{2+} binding component from the data. After transformation, Cd^{2+} burden data were then subjected to Michaelis-Menten analyses as described above.

K_m was also estimated on the basis of the free Cd^{2+} ion, substituted for Cd concentration in *Eq. 1*, as calculated by MINEQL+ (26). MINEQL+ is a geochemical equilibrium-modeling program that can be used to predict the chemical species present in aqueous systems given specific thermodynamic parameters, pH, and ion concentrations. MINEQL+ was used to determine the speciation of Cd in ^{109}Cd flux solutions (in PBS and Cl^--free PBS) (Table 1). Speciation analysis for the Cl^--free conditions necessitated input into the MINEQL+ database of a conditional stability constant for the Cd-gluconate complex of 1.15 as obtained from Fischer and Bipp (3). This log *K* value is based on a 1:1 complexation at near neutral pH.

Statistical methods. Data are presented as means ± SE (where *n* represents a cell population from one fish). The effects of gill cell subtype on Cd^{2+} or Ca^{2+} accumulation were tested for significant differences with a one-way ANOVA. Post hoc multiple comparisons were performed with Tukey's honestly significant difference test. A *P* value of 0.05 was considered statistically significant throughout. All statistical analyses were performed with SPSS (version 10).

RESULTS

In vivo ^{109}Cd exposures. In vivo Cd exposures at waterborne ^{109}Cd concentrations of 2.4 ± 0.1 μg/l were performed to determine the cellular localization of Cd^{2+} accumulation in isolated gill cell populations. The PNA^+ MR cells accumulated 94.2 ± 22.0 pg Cd^{2+} per 10^6 cells ($n = 11$), which represented from 2.7- to 12.1-fold more Cd^{2+} than taken up by the other isolated cells after the 1-h exposure (Fig. 1). The PNA^- MR cells accumulated only 25.8 ± 8.1 pg Cd^{2+} per 10^6 cells ($n = 12$), and the PV cells accumulated only 17.0 ± 5.2 pg Cd^{2+} per 10^6 cells ($n = 12$), amounts that were not significantly different ($P < 0.05$) from one another. In comparison, mucous cells accumulated only 7.2 ± 1.4 pg Cd^{2+} per 10^6 cells.

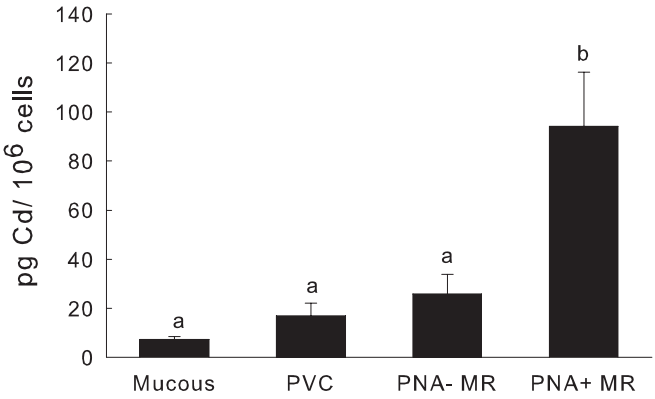

Fig. 1. ^{109}Cd accumulation for isolated mucous ($n = 8$), pavement (PV; $n = 12$), PNA^- mitochondria-rich (MR; $n = 12$), and PNA^+ MR ($n = 11$) cell populations isolated from the gill epithelia of adult rainbow trout exposed in vivo for 1 h to 2.4 ± 0.1 μg/l (means ± SE) Cd. Values are means ± SE in pg Cd^{2+} per 10^6 cells. Significant differences ($P < 0.05$) between treatment groups exist wherever common letters are not shared.

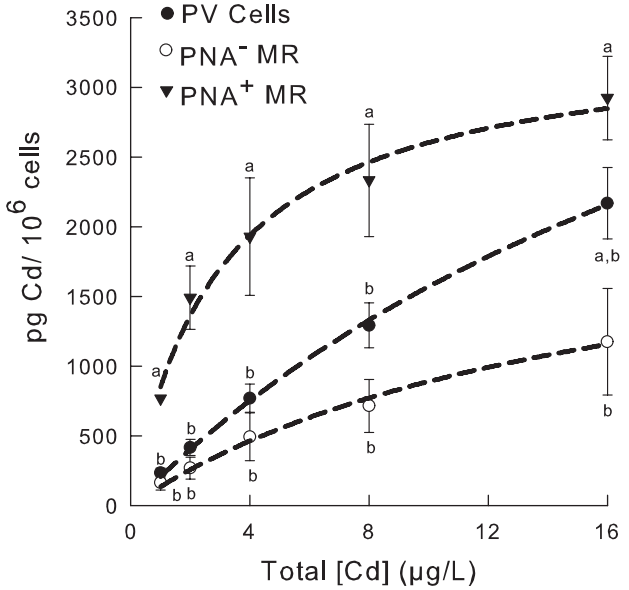

Fig. 2. Cd^{2+} accumulation at varying concentrations of ^{109}Cd in standard PBS for isolated PV ($n = 9$ for 1 μg/l; $n = 10$ for 2, 4, 8, and 16 μg/l ^{109}Cd), PNA^- MR ($n = 3$), and PNA^+ MR ($n = 3$) cell populations exposed under in vitro conditions for 60 s. Values are means ± SE in pg Cd^{2+} per 10^6 cells. Significant differences ($P < 0.05$) between treatment groups exist wherever common letters are not shared.

Cd speciation in different fluxing media using MINEQL+. The geochemical speciation program MINEQL+ (26) was used to determine the speciation of Cd in both standard PBS and Cl^--free PBS in Cd concentrations ranging from 1 to 16 μg/l (Table 1). In PBS, an estimated 14.6% of the total Cd was as the free Cd^{2+}. The remainder of the Cd was speciated into various cadmium chloride species, including $CdCl^+$, $CdCl_2$(aq), and $CdCl_3^-$. When Cl^- salts were replaced with their gluconate equivalents to make Cl^--free PBS, the precentage of the total Cd that was as the free Cd^{2+} increased to 83.1% at total Cd concentrations between 1 and 8 μg/l. This percentage decreased to 58.6% of the total at 16 μg/l Cd. The remaining Cd in the exposure medium was present as cadmium gluconate or $CdCO_3$.

In vitro ^{109}Cd exposures performed in standard PBS. ^{109}Cd in isolated gill cells was examined with an in vitro approach to better characterize the kinetics of Cd^{2+} accumulation. During in vitro ^{109}Cd exposures in PBS, PNA^+ MR cells accumulated the highest levels of Cd^{2+} (2,923 ± 299 pg per 10^6 cells; $n = 3$) compared with the other cell types after exposure to 16 μg/l Cd (Fig. 2). Michaelis-Menten analyses of the relationships between Cd^{2+} burden and total Cd concentration for the PNA^+ MR cells incubated in PBS gave a B_{max} of 3,375 ± 195 pg Cd^{2+} per 10^6 cells and a K_m of 3.0 ± 0.5 μg/l total Cd (27 nM). From this estimate of K_m, a log $K_{Cd\text{-}PNA+}$ of 7.57 was calculated for the total Cd in solution (see DISCUSSION for further comments). With the assumption that 14.6% of the total Cd in the PBS was in the free ionic form (Cd^{2+}) (Table 1), a log $K_{Cd\text{-}PNA+}$ of 8.41 (Cd^{2+}-specific accumulation) could be calculated for PNA^+ MR cells. The PNA^- MR cells accumulated ~50% less Cd^{2+} [1,176 ± 383 pg Cd^{2+} per 10^6 cells ($n = 3$)] than did the PNA^+ MR cells during exposure to 16 μg/l ^{109}Cd (Fig. 2). The PNA^- MR cells could also be described by Michaelis-Menten saturation kinetics; however, it was first necessary to subtract a small linear Cd accumulation component from Cd^{2+} cell burden values. The transformed data gave a B_{max} of 368 ± 156 pg Cd^{2+} per 10^6 cells and a K_m of 3.1 ± 2.0 μg/l Cd (28 nM) for the PNA^- MR cells. The PV cells also accumulated high amounts of Cd^{2+} (2,168 ± 255 pg per Cd^{2+} 10^6 cells) (Fig. 2), although Cd^{2+} accumulation did not appear to saturate over the Cd concentrations tested in the present study. Nonetheless, a B_{max} of 1,387 ± 462 pg Cd^{2+} per 10^6 cells and a K_m of 8.6 ± 2.8 μg/l Cd (77 nM) was estimated after a linear accumulation component was subtracted mathematically. Cd^{2+} accumulation was significantly higher in the PNA^+ MR cells at all concentrations (Fig. 2; $P < 0.05$).

In vitro ^{109}Cd exposures performed in Cl^--free PBS. Accumulation of Cd^{2+} in isolated gill cells was significantly reduced in all cell types when exposed to Cl^--free PBS (Fig. 3). In general, PV and PNA^+ MR cells continued to show relatively high levels of Cd^{2+} accumulation [1,639 ± 211 ($n = 13$) and 1,515 ± 264 ng Cd^{2+} per 10^6 cells ($n = 8$), respectively] after exposure to 16 μg/l ^{109}Cd. The PNA^- MR cells accumulated lower amounts of ^{109}Cd (941 ± 309 pg Cd^{2+} per 10^6 cells; $n = 9$). In all gill cell populations, Cd^{2+} uptake increased almost linearly with elevations in external Cd concentration (Fig. 3). Consequently, it was not possible to calculate B_{max} and K_m values for any of the three cell types when exposed to ^{109}Cd in Cl^--free PBS. Furthermore, ^{109}Cd accumulations in all cells were not significantly different from one another in this set of experiments (Fig. 3; $P < 0.05$). Figure 4 compares the absolute Cd^{2+} accumulation in all cell types after exposure to 16 μg/l ^{109}Cd in either PBS or Cl^--free PBS. The PV cells, PNA^- MR cells, and PNA^+ MR cells showed 24.4, 20.0, and 48.2% ($P < 0.05$) reductions in Cd^{2+} uptake, respectively, in Cl^--free PBS relative to those burdens obtained in standard PBS.

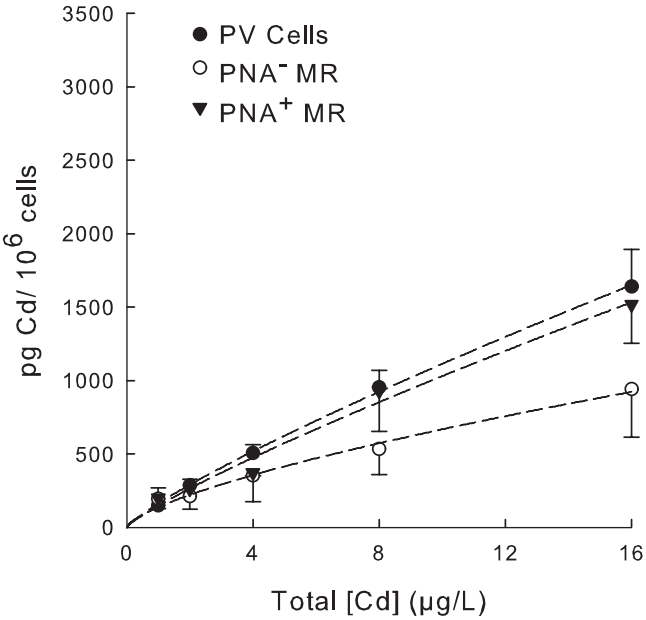

Fig. 3. Cd^{2+} accumulation at varying concentrations of Cd in Cl^--free PBS for isolated PV ($n = 11$ for 8 μg/l ^{109}Cd, and $n = 13$ for 1, 2, 4, and 16 μg/l ^{109}Cd), PNA^- MR ($n = 8$ for 1 μg/l ^{109}Cd; $n = 9$ for 2, 4, 8, and 16 μg/l ^{109}Cd), and PNA^+ MR ($n = 6$ for 1, 2, 4, and 8 μg/l ^{109}Cd; $n = 8$ for 16 μg/l ^{109}Cd) cells exposed under in vitro conditions for 60 s. Values are means ± SE in pg Cd^{2+} per 10^6 cells. No significant differences ($P < 0.05$) exist between any of the treatment groups.

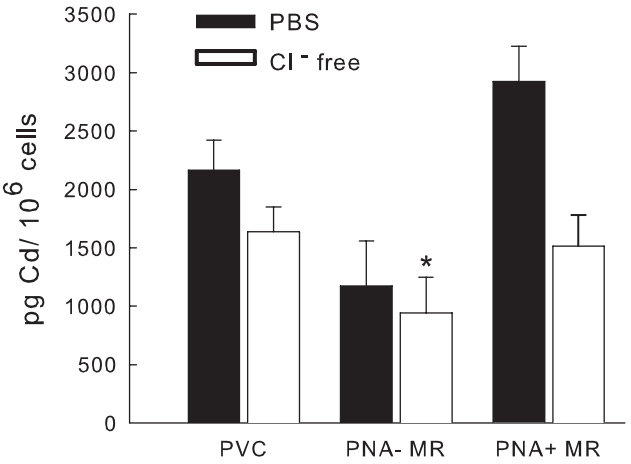

Fig. 4. ^{109}Cd accumulation in isolated gill cell fractions exposed for 60 s to 16 μg/l Cd in either standard PBS or Cl^--free PBS (standard PBS, $n = 10$ for PV cells and $n = 3$ for PNA^- MR and PNA^+ MR; for Cl^--free PBS, $n = 13$ for PV cells, $n = 9$ for PNA^- MR, and $n = 8$ for PNA^+ MR). Values are means ± SE in pg Cd^{2+} per 10^6 cells. *Significant difference between treatment groups ($P < 0.05$).

In vitro ^{45}Ca exposures performed in standard PBS. In vitro Ca^{2+} fluxes were performed on isolated gill cells at Ca concentrations ranging from 5 to 100 μM in PBS. Ca^{2+} uptake at 100 μM was approximately threefold higher in PNA^+ MR cells than found in either PNA^- MR or PV cells (Fig. 5*A*). Kinetic analysis for Ca^{2+} uptake in PNA^+ MR cells at total Ca concentrations below 20 μM demonstrated a high-affinity Ca^{2+} uptake pathway with a K_m of 4.73 μM and a B_{max} of 270 pmol Cd^{2+} per 10^6 cells (Fig. 5*B*).

DISCUSSION

Differential Cd^{2+} and Ca^{2+} transport. Recent studies have identified the PNA^- MR cell type as the site of active Na^+ transport (25) and H^+ excretion during intracellular acidification (4, 25). However, up to now, it has been unclear whether functional separation of other ion transport processes also exists between these two MR cell types. In the current study, we provide evidence that the apical entry of Cd^{2+} and Ca^{2+} in the gill epithelium of rainbow trout occurs preferentially in a specific subtype of MR, termed the PNA^+ MR cell. Although this study is not the first to propose the heterogeneous uptake of these ions in the MR cells of the freshwater fish gill (31), it is the first to provide definitive quantitative evidence to this effect. Our present study found an approximately three- to fourfold greater Cd^{2+} accumulation in PNA^+ MR cells than in PV cells or in PNA^- MR cells after in vivo Cd exposures (Fig. 1). In the study by Wicklund Glynn et al. (31), the authors demonstrated ^{109}Cd sequestration in a "subpopulation" of MR cells on the gill filament, as assessed by autoradiographic techniques. This is in stark contrast to the general belief that Cd^{2+} is accumulated in all MR cells. Relative to the high Cd^{2+} accumulation in PNA^+ MR cells after in vivo exposures, PV cells and PNA^- MR cells showed relatively low metal burdens (Fig. 1).

In contrast to results obtained during the in vivo Cd exposures, PV cells showed unexpectedly high levels of Cd^{2+} accumulation during in vitro exposures. Although it is presently unclear why a difference in Cd^{2+} accumulation in PV cells existed between the in vivo and in vitro exposures, it may have been associated with the loss of polarity in gill cells after dissociation of the intact gill epithelium. Digestion of the gill epithelium to yield dispersed gill cells would cause transport proteins on both the apical and basolateral membranes to become equally available for ^{109}Cd transport. As a result, ion channels on the basolateral surface of PV cells, which would normally not be exposed to waterborne Cd, would subsequently become available for Cd^{2+} transport. In finding high accumulation of ^{109}Cd in PV cells only during in vitro Cd incubations (Figs. 2 and 3) and not during in vivo exposures (Fig. 1), it is feasible that putative Cd^{2+} and Ca^{2+} transporters are specifically located on the basolateral surfaces alone of PV cells, thus allowing for the inward movement of Cd^{2+}. The presence of such transporters would help explain why Cd^{2+} fed in the diet can accumulate in the gill tissue (28). Although the exact nature of these putative Cd^{2+} transport sites is unknown, Cd^{2+} uptake exhibited an extensive linear component with increasing amounts of extracellular Cd^{2+}.

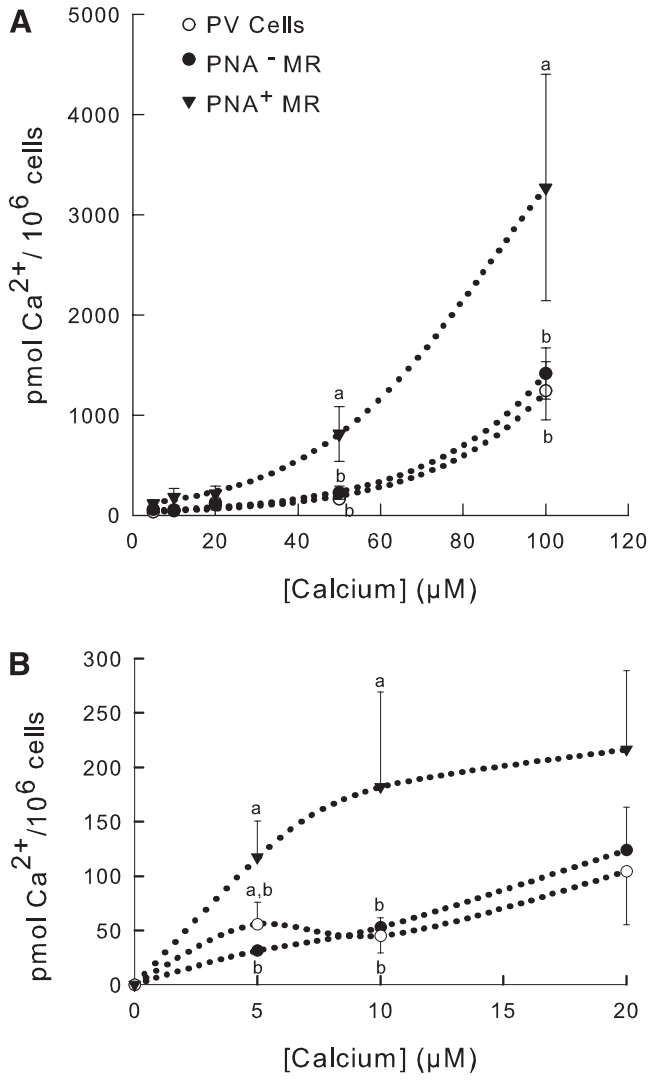

Fig. 5. Ca^{2+} accumulation at varying concentrations of Ca ranging from 0 to 100 μM (*A*) or 0 to 20 μM (*B*) in standard PBS for isolated PV ($n = 9$), PNA^- MR ($n = 9$), and PNA^+ MR ($n = 4$) cell populations exposed in in vitro conditions for 30 min. Values are means ± SE in pmol Ca^{2+} per 10^6 cells. *Significant difference between the other 2 treatment groups ($P < 0.05$).

Although it is known that inorganic Cd complexes such as $CdCl_2$ are not readily taken up by fish from water (16), we wanted to nonetheless test whether ^{109}Cd was accumulating in PV cells during in vitro exposures because of passive transport of $CdCl_2$ complexes. According to the speciation analyses by MINEQL+, only 14.6% of the total Cd in PBS would theoretically exist as Cd^{2+} (Table 1). The remainder of the Cd would be expected to form various $CdCl_2$ complexes. Thus we repeated the in vitro Cd^{2+} fluxes using a Cl^--free PBS instead of the standard PBS, by replacing KCl and NaCl with potassium gluconate and sodium gluconate, respectively. Gluconate is less readily able to complex with Cd^{2+}. Furthermore, the cadmium gluconate complex is a larger molecule than the $CdCl_2$ species and is, hence, less likely to diffuse across plasma membranes. If, in fact, passive diffusion of $CdCl_2$ complexes did account for the high uptake of Cd in PV cells, it would be expected that the absence of $CdCl_2$ species would greatly reduce Cd accumulation in this cell type. Meanwhile, the concomitant increase of the free Cd^{2+} concentration in the Cl^--free fluxing medium (at 1–8 μg/l total Cd concentration) might be expected to enhance Cd^{2+} accumulation in the PNA^+ MR cells. In other words, because Cd^{2+} is the chemical form of Cd thought to permeate epithelial Ca channels (30), Cd^{2+} accumulation in PNA^+ MR cells should be saturated at a much lower concentration of total Cd. In fact, the opposite was true. Exposure of cells to Cd under Cl^--free conditions had its largest inhibitory effect on ^{109}Cd accumulation in the PNA^+ MR cells. Furthermore, the transport kinetics of Cd^{2+} became approximately linear (Fig. 3), and ^{109}Cd accumulation was reduced by up to 48% at 16 μg/l Cd exposure in Cl^--free PBS (Fig. 4). The mechanistic basis for this Cl^- dependency of Cd^{2+} transport is presently not known. PNA^+ MR cells are believed to be the site of apical Cl^-/HCO_3^- exchange (19). Removal of Cl^- has been shown to increase the intracellular pH of other cell types expressing apical Cl^-/HCO_3^- exchange (27). Clearly, further studies are needed to study the potential link between acid-base regulation and Cd^{2+} transport. Another possibility is that replacement of Cl^- with various gluconate salts could possibly produce different cadmium-gluconate complexes such as Cd^{2+}-gluconate-hydroxide and others, which are currently not considered within MINEQL+ because of the unavailability of stability constants for these putative complexes. If Cd^{2+} was, in fact, slightly reduced rather than increased by the addition of gluconate to the system, the greatest inhibitory effect on Cd^{2+} binding would occur in the PNA^+ MR cells because of the shape of its kinetic curve (Fig. 2).

Another aim of the present study was directed at determining the cellular localization for the apical entry of Ca^{2+} uptake in the freshwater fish gill. Unlike with the set of ^{109}Cd experiments, it was only possible to obtain reliable uptake rates from in vitro fluxes because of the low levels of ^{45}Ca in gill cell populations after in vivo exposures. Consequently, we decided to perform in vitro Ca^{2+} fluxes at relatively low concentrations (≤100 μM), because of the likelihood that apical Ca^{2+} uptake pathways, which can transport Ca^{2+} from water at low ion levels, might be the primary route of Ca^{2+} uptake targeted in our experiments. In other words, by performing these in vitro experiments at such low Ca^{2+} levels, the possibility of Ca^{2+} being taken up by lower affinity basolateral Ca^{2+} transport proteins would be attenuated. Using this approach, we were able to find a high-affinity Ca^{2+} uptake pathway in PNA^+ MR cells (K_m ~4 μM) that was not evident in either the PNA^- MR and PV cells. Increasing the Ca concentrations between 20 and 100 μM produced an additional increase in Ca^{2+} uptake in all cell types, although its magnitude was again most pronounced in the PNA^+ MR cells. Although we cannot unequivocally prove that the uptake of Ca^{2+} in the PNA^+ MR cells is via proteins on the apical membrane, the fact that Cd^{2+} is taken up by this route (as shown by the in vivo data) suggests that the PNA^+ MR cell is the primary site for the apical entry of Ca^{2+} at the fish gill.

The significance of the high-affinity saturable component in the PNA^+ MR cells occurring at concentrations below 20 μM is unclear (Fig. 5*B*). Perry and Wood (22) calculated the K_m value for Ca^{2+} uptake for adult rainbow trout at ~140 μM, suggesting the high-affinity uptake pathway (K_m of 4.73 μM sites) in the PNA^+ MR cells is not likely associated with transepithelial Ca^{2+} uptake. The K_m for Ca^{2+} uptake (22) is at a concentration slightly above those used in the present study, which may explain why saturation was not achieved between 20 and 100 μM. Nonetheless, increasing the concentration over this range produced a marked secondary increase in Ca^{2+} uptake in all cell types, especially in the PNA^+ MR cells.

Perry and Wood (22) found that ^{45}Ca taken up by the gills of freshwater rainbow trout passed into the arterio-arterial circulation, correlating with the relative abundance of lamellar MR cells. In contrast, Ishihara and Mugiya (11) used an oxalate-based method to localize Ca^{2+} uptake to the MR cells of the goldfish gill, which in this species was most prominent in the filamental epithelium rather than in the lamellar epithelium. Our finding that preferential Ca^{2+} uptake occurs in the PNA^+ MR cell, which has been previously shown to localize to the filamental epithelium of the fish gill (5), is in agreement with the findings of Ishihara and Mugiya (11). However, when considering the relative importance of each of the specific cell types, it is important to consider the abundance of the different cell populations in the gill epithelium in vivo. Because PV cells are by far the most abundant cell type (80–95%) in the gill epithelium (21), this may result in these cells having a significant contribution to transepithelial Ca^{2+} and Cd^{2+} flux in vivo, despite the fact that PV cells possess low absolute uptake rates of both ^{109}Cd (in vivo exposure only) and ^{45}Ca (in vitro exposures only). Certainly, the earlier work of Zia and McDonald (34) would support this statement. Furthermore, it is important to note that, on the basis of previous studies, PNA^+ MR cells represent only between 20 and 40% of the total MR cells in the gill epithelium (7, 25). Considering the already low abundance of MR cells in the gill epithelium in vivo (2, 6, 19), the much greater number of PV cells could, in fact, make a large contribution to the overall transepithelial Ca^{2+} and Cd^{2+} flux.

Kinetics. In examining the kinetics of Cd^{2+} accumulation in the PNA^+ fraction, we obtained a log $K_{Cd\text{-}gill\ PNA}$ value of 7.57 based on total Cd and 8.41 based on ionic Cd^{2+}. These values are extremely similar to those obtained in studies of Cd transport in whole gills after in vivo exposures. For example, Hollis et al. (8) obtained a log $K_{Cd\text{-}gill}$ of 7.6 during Cd exposures in hard water and log $K_{Cd\text{-}gill}$ of 7.3 (9) for rainbow trout in soft water, whereas Playle et al. (24) produced a log $K_{Cd\text{-}gill}$ of 8.6 for fathead minnows exposed to Cd in soft water. In the above studies, conditional stability constants (log K values) for metal binding to the fish gill were based on the

theoretical Cd^{2+} concentration in the water. The similarity between our log $K_{Cd\text{-}gill}$ values and those for freshwater fish in vivo strongly supports the validity of the kinetic results of our in vitro work.

Perspectives

In this study, the Cd concentrations used (1–16 μg/l) were of environmental relevance. According to the Canadian Water Quality Guidelines (1), a maximum of 5 μg Cd/l is allowed for the protection of freshwater life exposed chronically to Cd in hard water. Furthermore, the concentrations of Cd used in both the in vivo and in vitro experiments are comparable to the range of Cd concentrations used in previous metal binding and toxicity studies (reviewed in Ref. 33).

There is evidence that the relative proportion and functional characteristics of the MR cell subtypes studied here are influenced by alterations in environmental salinity (7), cortisol treatment (5), and acid-base disturbances (4, 25). Respiratory alkalosis or acidosis can, for example, alter cell-type ratios in the fish gill to maintain acid-base homeostasis (2, 6, 12, 17). In turn, changes in physiology can affect the susceptibility of fish to metals. If different gill cell populations do, indeed, possess different roles in ion transport and acid-base homeostasis, stressors that alter the relative abundance of these cell types on the gill epithelium may increase or decrease the uptake and toxicity of metals such as Cd under different environmental conditions.

GRANTS

This work was supported by an Natural Sciences and Engineering Research Council of Canada Discovery Grant to C. M. Wood. C. M. Wood is also supported by the Canada Research Chair Program.

REFERENCES

1. **Canadian Council of Ministers of the Environment.** *Canadian Water Quality Guidelines*. Winnipeg, Manitoba, 1999.
2. **Evans DH.** The fish gill: site of action and model for toxic effects of environmental pollutants. *Environ Health Perspect* 71: 47–58, 1987.
3. **Fischer B and Bipp HP.** Removal of heavy metals from soil components and soils by natural chelating agents. Part II. Soil extraction by sugar acids. *Wat Air Soil Poll* 138: 271–288, 2002.
4. **Galvez F, Reid SD, Hawkings G, and Goss GG.** Isolation and characterization of mitochondria-rich cell types from the gill of freshwater rainbow trout. *Am J Physiol Regul Integr Comp Physiol* 282: R658–R668, 2002.
5. **Goss GG, Adamia S, and Galvez F.** Peanut lectin binds to a subpopulation of mitochondria-rich cells in the rainbow trout gill epithelium. *Am J Physiol Regul Integr Comp Physiol* 281: R1718–R1725, 2001.
6. **Goss GG, Perry SF, Fryer JN, and Laurent P.** Gill morphology and acid-base regulation in freshwater fishes. *Comp Biochem Physiol* 119A: 107–115, 1998.
7. **Hawkings GS, Galvez F, and Goss GG.** Seawater acclimation causes independent alterations in Na^+/K^+- and H^+-ATPase activity in isolated mitochondria-rich cell subtypes of the rainbow trout gill. *J Exp Biol* 207: 905–912, 2004.
8. **Hollis L, McGeer JC, McDonald DG, and Wood CM.** Cadmium accumulation, gill Cd binding, acclimation, and physiological effects during long term sublethal Cd exposure in rainbow trout. *Aquat Toxicol (Amst)* 46: 101–119, 1999.
9. **Hollis L, McGeer JC, McDonald DG, and Wood CM.** Effects of long term sublethal Cd exposure in rainbow trout during soft water exposure: implications for biotic ligand modeling. *Aquat Toxicol (Amst)* 51: 93–105, 2000.
10. **Hollis L, McGeer JC, McDonald DG, and Wood CM.** Protective effects of calcium against chronic waterborne cadmium exposure to juvenile rainbow trout. *Environ Toxicol Chem* 19: 2725–2734, 2000.
11. **Ishihara A and Mugiya Y.** Ultrastructural evidence of calcium uptake by chloride cells in the gills of goldfish, *Carassius auratus*. *J Exp Zool* 242: 121–129, 1987.
12. **Marshall WS.** Na^+, Cl^-, Ca^{2+} and Zn^{2+} transport by fish gills: retrospective review and prospective synthesis. *J Exp Zool* 293: 264–283, 2002.
13. **Marshall WS, Bryson SE, Burghardt JS, and Verbost PM.** Ca^{2+} transport by opercular epithelia of the fresh water adapted euryhaline teleost, *Fundulus heteroclitus*. *J Comp Physiol [B]* 165: 268–277, 1995.
14. **Marshall WS, Bryson SE, and Wood CM.** Calcium transport by isolated skin of rainbow trout. *J Exp Biol* 166: 297–316, 1992.
15. **McCormick SD, Hasegawa S, and Hirano T.** Calcium uptake in the skin of a freshwater teleost. *Proc Natl Acad Sci USA* 89: 3635–3638, 1992.
16. **Pärt P, Svanberg O, and Kiessling A.** The availability of cadmium to perfused rainbow trout gills in different water qualities. *Water Res* 19: 427–434, 1985.
17. **Perry SF.** The chloride cell: structure and function in the gills of freshwater fishes. *Annu Rev Physiol* 59: 325–347, 1997.
18. **Perry SF and Flik G.** Characterization of branchial transepithelial calcium fluxes in freshwater trout gill. *J Exp Zool* 216: 345–347, 1988.
19. **Perry SF, Goss GG, and Fenwick JC.** Interrelationships between gill chloride cell morphology and calcium uptake in freshwater teleosts. *Fish Physiol Biochem* 10: 327–337, 1992.
20. **Perry SF, Shahsavarani A, Georgalis T, Bayaa M, Furimsky M, and Thomas SL.** Channels, pumps, and exchangers in the gill and kidney of freshwater fishes: their role in ionic and acid-base regulation. *J Exp Zool* 300: 53–62, 2003.
21. **Perry SF and Walsh PJ.** Metabolism of isolated fish gill cells: contribution of epithelial chloride cells. *J Exp Biol* 144: 507–520, 1989.
22. **Perry SF and Wood CM.** Kinetics of branchial calcium uptake in the rainbow trout: effects of acclimation to various external calcium levels. *J Exp Biol* 116: 411–433, 1985.
23. **Pisam M, Caroff A, and Rambourg A.** Two types of chloride cells in the gill epithelium of a freshwater-adapted euryhaline fish: *Lebistes reticulatus*; their modifications during adaptation to saltwater. *Am J Anat* 197: 40–50, 1987.
24. **Playle RC, Dixon DG, and Burnison K.** Copper and cadmium binding to fish gills: estimates of metal-gill stability constants and modelling of metal accumulation. *Can J Fish Aquat Sci* 50: 2678–2687, 1993.
25. **Reid SD, Hawkings GS, Galvez F, and Goss GG.** Localization and characterization of phenamil-sensitive Na^+ influx in isolated rainbow trout gill epithelial cells. *J Exp Biol* 206: 551–559, 2003.
26. **Schecher WD and McAvoy DC.** MINEQL+: a chemical equilibrium program for personal computers (version 4.5). Hallowell, ME: Environmental Research Software, 2001.
27. **Sterling D and Casey JR.** Transport activity of AE3 chloride/bicarbonate anion-exchange proteins and their regulation by intracellular pH. *Biochem J* 344: 221–229, 1999.
28. **Szebedinszsky C, McGeer JC, McDonald DG, and Wood CM.** Effects of chronic Cd exposure via the diet or water on internal organ-specific distribution and subsequent gill Cd uptake kinetics in juvenile rainbow trout. *Environ Toxicol Chem* 20: 597–607, 2001.
29. **Verbost PM, Flik G, Lock RAC, and Wendelaar Bonga SE.** Cadmium inhibition of Ca^{2+} uptake in rainbow trout gills. *Am J Physiol Regul Integr Comp Physiol* 253: R216–R221, 1987.
30. **Verbost PM, VanRooij J, Flik G, Lock RAC, and Wendelaar Bonga SE.** The movement of cadmium through freshwater trout branchial epithelium and its interference with calcium transport. *J Exp Biol* 145: 185–197, 1989.
31. **Wicklund Glynn A, Norrgren L, and Müssener Å.** Differences in uptake of inorganic mercury and cadmium in the gills of the zebrafish, *Brachydanio rerio*. *Aquat Toxicol (Amst)* 30: 13–26, 1994.
32. **Wicklund A and Runn P.** Calcium effects on cadmium uptake, redistribution, and elimination in minnow, *Phoxinus phoxinus*, acclimated to different calcium concentrations. *Aquat Toxicol (Amst)* 13: 109–122, 1988.
33. **Wood CM.** Toxic responses of the gill. In: *Target Organ Toxicity in Marine and Freshwater Teleosts*, edited by Schlenk D and Benson WH. London: Taylor & Francis, 2001, p. 1–89.
34. **Zia S and McDonald DG.** Role of the gills and gill chloride cells in metal uptake in the freshwater-adapted rainbow trout, *Oncorhynchus mykiss*. *Can J Fish Aquat Sci* 51: 2482–2492, 1994.